

Membrane Activity of Biomimetic Facially Amphiphilic Antibiotics<sup>†</sup>Lachelle Arnt,<sup>‡</sup> Jason R. Rennie,<sup>‡</sup> Sebastian Linser,<sup>§</sup> Regine Willumeit,<sup>\*,§</sup> and Gregory N. Tew<sup>\*,‡</sup>*Polymer Science and Engineering Department, University of Massachusetts, Amherst, 120 Governors Drive, Amherst, Massachusetts 01003, and GKSS Research Center, Max-Planck-Strasse 1, 21502 Geesthacht, Germany**Received: August 4, 2005; In Final Form: December 9, 2005*

Membranes are a central feature of all biological systems, and their ability to control many cellular processes is critically important. As a result, a better understanding of how molecules bind to and select between biological membranes is an active area of research. Antimicrobial host defense peptides are known to be membrane-active and, in many cases, exhibit discrimination between prokaryotic and eukaryotic cells. The design of synthetic molecules that capture the biological activity of these natural peptides has been shown. In this report, the interaction between our biomimetic structures and different biological membranes is reported using both model vesicle and in vitro bacterial cell experiments. Compound **1** induces 12% leakage at 20  $\mu\text{g/mL}$  against phosphatidylglycerol (PG)–phosphatidylethanolamine (PE) vesicles vs only 3% leakage at 200  $\mu\text{g/mL}$  against phosphatidyl-L-serine (PS)–phosphatidylcholine (PC) vesicles. Similarly, a 40% reduction in fluorescence is measured in lipid movement experiments for PG–PE compared to 10% for PS–PC at 600 s. A 30 °C increase in the phase transition of stearoyl-oleoyl-phosphatidylserine is observed in the presence of **1**. These results show that lipid composition is more important for selectivity than overall net charge. Additionally, the overall concentration of a given lipid is another important factor. An effort is made to connect model vesicle studies with in vitro data and naturally occurring lipid compositions.

## Introduction

The interaction of molecules with lipid membranes is of critical importance as many cellular mechanisms are regulated by transmembrane macromolecules. The ability of amphiphilic molecules to insert into membranes is an active area of research, and one recent example includes the development of host defense peptide (HDP) mimics.<sup>1</sup> These mimics, like their natural analogues, are designed to be membrane-active, ultimately leading to cell death. More specifically, the peptides and many of their structural derivatives, including recent mimics such as  $\beta$ -peptides,<sup>2–6</sup> peptoids,<sup>7</sup> cyclic and noncyclic D,L amino acids,<sup>8,9</sup> arylamides,<sup>10</sup> and phenylene ethynyls,<sup>11</sup> are able to discriminate between prokaryotic and mammalian red blood cell (RBC) membranes. Many of the previously developed HDP mimics also focused on capturing the overall helical architecture,<sup>2,6,7</sup> while our work has focused solely on deconvoluting the helical architecture from the facially amphiphilic (FA) design.<sup>11–14</sup> These results showed convincingly that the helical architecture is not a requirement for active and selective mimics. Having succeeded in this endeavor, attempts to understand their interactions with lipid membranes have been under investigation and are reported here.

The design principles implicit in developing HDP mimics are highlighted in Figure 1 with a cartoon meant to capture the spatial arrangement of charged, polar (P), and nonpolar (NP) groups. This overall architecture has been described previously as FA since the P and NP groups are located on opposite sides

of the molecular backbone and represents a significantly different architecture<sup>15,16</sup> from traditional amphiphiles such as lipids and surfactants. Molecules that are FA have their P and NP groups segregated along opposite faces of the overall one-dimensional (1-D), two-dimensional (2-D), or three-dimensional (3-D) structure. For example, the molecules described here represent 1-D examples, while an amphipathic  $\alpha$ -helix would be 2-D, and folded structures such as defensin are 3-D.<sup>17</sup> In all cases, these molecules have faces, or large surface areas, that are either charged or nonpolar. Figure 1 also shows the structures of two compounds, prepared in our laboratory, which are potentially antimicrobial as well as selective toward bacteria over human red blood cells. The two molecules, although similar in overall size and molecular weight (MW), represent the extremes of design. The all-carbon backbone, phenylene ethynylene **1**, has no intramolecular interactions, such as hydrogen bonding, which would limit conformational freedom, while the arylamide, **2**, is conformationally rigid due to intramolecular hydrogen bonding and negative design elements such as steric repulsion between the carbonyl oxygens and pyrimidine nitrogens. Only the interaction of **1** with lipids is discussed here for simplicity since **2** behaves very similarly in all experiments to date.

The interfacial, or lipid membrane, activity of HDPs is well-known, although much more remains to be learned about the details of binding, insertion, and transport across the membrane. Even more interesting is the fact that these molecules and their mimics demonstrate selectivity between prokaryotic and eukaryotic cells. The origin of this selectivity is believed to rise from favorable interactions with certain lipids as the composition of molecules that make up the membrane can be quite different among cell types.<sup>18–20</sup> In addition, bacterial cells are more negatively charged than RBCs.<sup>21–23</sup> The ability of these

<sup>†</sup> Part of the special issue "Michael L. Klein Festschrift".<sup>\*</sup> Authors to whom correspondence should be addressed. E-mail: Regine.Willumeit@gkss.de; tew@mail.pse.umass.edu.<sup>‡</sup> University of Massachusetts, Amherst.<sup>§</sup> GKSS Research Center.

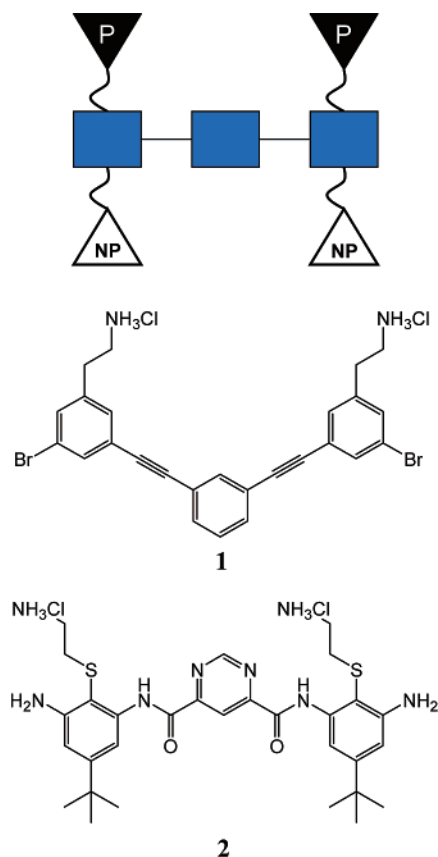


**Figure 1.** Spatial arrangement of polar and nonpolar groups critical for host defense peptides. The ability to transfer this design to simple abiotic molecules would enable novel antimicrobial compounds. Top panel: A schematic diagram representing a facially amphiphilic architecture in which polar and nonpolar groups segregate to opposite faces of the molecular backbone. Bottom panel: Two oligomeric compounds designed to capture the essential physiochemical features of host defense peptides.

molecules to discriminate between membranes is truly remarkable. As a result, gaining a better understanding of how these FA molecules interact with lipids is important fundamentally and practically. Important progress in this area will involve continued development of synthetic analogues, which allow much more structural diversity than peptides, and more detailed computational investigations on their membrane activity.

Simulations of membrane-active peptides have increased over the last several years.<sup>24–28</sup> Recently, Klein and co-workers reported molecular dynamics (MD) simulations exploring the fundamental mechanisms of membrane insertion for amphiphilic molecules such as those reported here.<sup>29–33</sup> Using a coarse grain (CG) model, they simulated the binding, insertion, and transport of an amphiphilic nanotube—dimyristoylphosphatidylcholine (DMPC) system.<sup>29</sup> This method allows events with longer time scales (nano- to microseconds) to be studied and their results show that binding is spontaneous with the nanotube parallel to the lipid membrane followed by transport, which is chaperoned by lipids, into the membrane. Near atomistic details can be obtained including the equilibrium value for area per headgroup, which decreases from  $\sim 70$  to  $49 \text{ \AA}^2$ , during insertion, to  $54 \text{ \AA}^2$  after complete insertion into the hydrophobic core of the membrane and finally to  $56 \text{ \AA}^2$  upon complete rotation of the nanotube perpendicular to the membrane.<sup>29</sup> It appears that the positively charged residues adhere to negatively charged lipids.<sup>29</sup> The role of the cationic groups present in HDPs and the

biomimetic structures reported here remains to be studied in detail;<sup>34</sup> however, it can be expected that similar interactions will occur.<sup>29</sup>

In this report, we describe the interaction of FA molecules with lipid membranes in four different experiments. These studies show that lipid composition of the membrane greatly impacts the level of interaction, which may have important consequences on biological selectivity. It is known that the lipid composition of bacterial and eukaryotic cells differ significantly.<sup>18,35</sup> Bacterial membranes contain negatively charged phospholipids such as phosphatidylglycerol (PG) and cardiolipin as well as the zwitterionic phospholipid phosphatidylethanolamine (PE).<sup>19,20,36</sup> The outer membrane of gram-negative bacteria contains a large amount of polyanionic lipopolysaccharides.<sup>37</sup> In contrast, the outer leaflets of mammalian cell membranes are neutral at physiological pH and mainly composed of phosphatidylcholine (PC), PE, sphingomyelin, and cholesterol.<sup>38,39</sup> Human RBCs do contain a relatively small amount of the negatively charged phosphatidyl-L-serine (PS); however, it is usually confined to the inner leaflet.<sup>39</sup> In addition to lipid composition, lipid ordering within the membrane can have a significant influence on how molecules interact.

Our experiments show that lipid composition greatly impacts the membrane activity of these FA biomimetics. Vesicle leakage and lipid movement experiments demonstrate that PG–PE systems are much more sensitive to the presence of **1** than PS–PC. Direct action against the plasma membrane of *Staphylococcus aureus* shows strong leakage and supports the membrane activity observed in vesicle studies. X-ray studies demonstrate that binding to pure PS is favorable compared to PC, suggesting that the dilution of this lipid with other molecules, like PC, helps explain the lack of activity in PC–PS vesicles.

## Experimental Section

The activities of these compounds were evaluated using standard methods.<sup>40</sup> Briefly, the compounds were dissolved in dimethylsulfoxide (DMSO) or buffered water to make stock solutions. The stock solution was then diluted into 96-well plates and diluted with Mueller Hinton (MH) medium to a constant volume. All bacteria were either taken from stock glycerol solutions or from a frozen stock, diluted into MH medium, and grown overnight at  $37^\circ\text{C}$ . Subsamples of these cultures were grown for 3 h, the  $\text{OD}_{600}$  was measured, and then the cells were diluted to  $0.001 \text{ OD}_{600}$ . The diluted cell solutions (approximately  $10^5$  cells/mL) were added to the 96-well plate and incubated at  $37^\circ\text{C}$  for 6 h. The minimal inhibitory concentration (MIC) value reported is the minimum concentration necessary to inhibit 90% of the cell growth. This was determined by measuring cell growth at  $\text{OD}_{600}$  after 6 h in 2-fold serial dilutions of **1** following standard protocols. The MIC of **1** and **2** against *Escherichia coli* D31 is  $0.8 \mu\text{g/mL}$  and against *S. aureus* ATCC 25923 is  $0.8 \mu\text{g/mL}$ . The MIC of MSI-78, a Magainin derivative, against the same *E. coli* strain was  $12.0 \mu\text{g/mL}$ . The hemolysis ( $\text{HC}_{50}$ ) values, or 50% leakage of hemoglobin from RBCs, were determined to be 75 and  $18 \mu\text{g/mL}$  for **1** and **2**, respectively. This gives a selectivity of 94 for **1** and 22 for **2** compared to 10 for MSI-78.

**Vesicle Leakage.** Vesicles were prepared using the film rehydration method.<sup>41</sup> The desired amount of lipid solution was transferred to a glass vial and dried using nitrogen to form a thin film on the wall of the vial. Either buffer or calcein solution (40 mM calcein in pH 7 10 mM  $\text{Na}_2\text{PO}_4$  buffer) was added to the lipid film to a final concentration of  $10 \mu\text{mol lipid/mL}$  of solution. The solution was then warmed in water and frozen in

acetone/liquid nitrogen for three cycles and then sonicated for 15 min. This procedure was repeated for another sonication cycle, ultimately ending with freezing and warming the solution. In the case of the encapsulated calcein vesicles, the vesicles were then run through a size exclusion Sephadex G-25 column to remove the excess dye and collect the vesicles. All vesicles were used within 2 days.

Calcein leakage experiments were performed by using vesicles in a pH 7.0 10 mM  $\text{Na}_2\text{PO}_4$  buffered solution and adding various amounts of polymer in DMSO.<sup>42</sup> Emission at 515 nm was monitored over time. The excitation wavelength was 490 nm. The percentage of DMSO in any experiment was less than 4%. Control experiments with 5% DMSO demonstrated that the vesicles were not lysed by the presence of DMSO. After the fluorescence of the polymer was monitored, 50  $\mu\text{L}$  of 0.2% Triton X-100 was added to determine the intensity at 100% lysis.

**Lipid Movement.** The lipid movement experiments were performed by using asymmetrically labeled vesicles.<sup>43</sup> In this case, the vesicles were prepared using 0.5 mol % headgroup 7-nitro-2,1,3-benzoxadiazol-4-yl (NBD)-PS lipids to make symmetrically labeled vesicles. The NBD fluorescence of the outer leaflet of the vesicle was quenched by dithionite reduction by adding 75  $\mu\text{L}$  of 1 M sodium hydrosulfite/1 M Tris to 1 mL of vesicles at a time and allowing incubation for 15 min. The fraction of the NBD lipids that had moved from the inner to the outer leaflet of the vesicles with the addition of the active compound was determined by dithionite quenching. The asymmetric vesicles (25  $\mu\text{L}$ ) were added to buffer (1 mL). Approximately 10  $\mu\text{L}$  of quencher solution was added to the 1.025  $\mu\text{L}$  solution to make a total volume of 1.035  $\mu\text{L}$ . To this solution, varying concentrations of the active compound were added from a stock solution of 2 mg/mL, keeping the DMSO concentration less than 5%. DMSO did not have an effect on lipid movement as determined by adding pure DMSO at concentrations up to 5%. The fluorescence was monitored at 530 nm (exciting at 450). The resulting fluorescence values were compared to the intensity of the vesicle solution prior to addition of the active agent.

**In Vitro Dye Leakage.** Cytoplasmic membrane permeability was measured using the membrane-potential-sensitive cyanine dye diSC3-5.<sup>23,44–48</sup> This dye is known to distribute between the cells and the medium depending on the membrane potential. Once the dye is inside the membrane, it aggregates and self-quenches. With the addition of a membrane-permeabilizing agent, the dye is released and fluorescence over time can be monitored. In this experiment, *S. aureus* ATCC 25923 was used and grown at 37°C with shaking until mid-logarithmic phase. The cells were collected by centrifugation, washed once with buffer (5 mM HEPES, pH 7, 5 mM glucose), and resuspended to an optical density ( $\text{OD}_{600}$ ) of 0.05. The cells were incubated with 0.4  $\mu\text{M}$  diSC3-5 for an hour for maximal uptake of the dye after which 100 mM KCl was added to equilibrate the cytoplasmic and external potassium ion concentration. The cells were mixed with the concentration of active compound desired, and the fluorescence was monitored using a Perkin-Elmer model LS5 spectrophotometer with an excitation wavelength of 622 nm and an emission wavelength of 670 nm. Dye release upon addition of 1% DMSO was monitored as a control since DMSO was kept at concentrations below 1% throughout the experiment. There was no observed dye release upon addition of DMSO, so it is not shown.

**Lipid Organization.** The phospholipids were dissolved in methanol/chloroform (1:2, by volume), the solvent was then

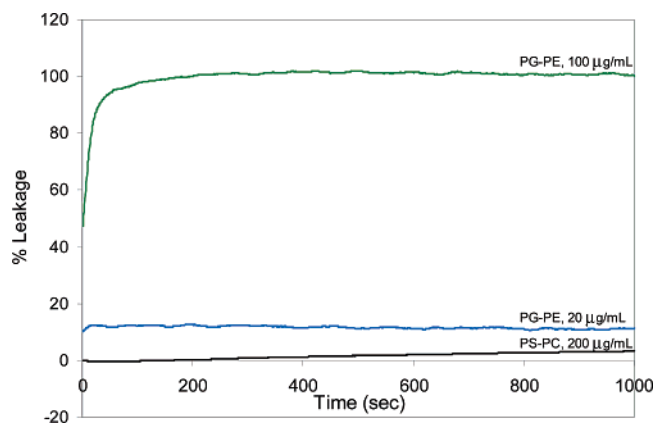


**Figure 2.** Two different calcein-loaded vesicle systems prepared with 10 mol % negatively charged phospholipids but composed of different lipid headgroups. The percent leakage of calcein was monitored upon addition of **1**. In each experiment, complete leakage was obtained by the addition of Triton X-100 as a control. The PG-PE vesicles showed significantly more leakage than the corresponding PS-PC vesicles. For example, when 20  $\mu\text{g/mL}$  of **1** was added to PG-PE vesicles 12% leakage was observed, while 200  $\mu\text{g/mL}$ , or 10 times more, of **1** only produced 3% leakage from PC-PS vesicles.

removed slowly by a constant stream of nitrogen, and the resulting lipid film was dried under vacuum overnight. The lipid films were hydrated in buffer (10 mM sodium phosphate, 90 mM NaCl, pH 7.4, final concentration 25 mg/mL) and heated for 2–4 h above the temperature for the  $\text{L}\beta \rightarrow \text{L}\alpha$  phase transition (transition temperature 17 °C) with repeated vortexing (1 min) every 30 min of incubation time. For lipid/**1** mixtures (10:1 molar ratio) the respective amount of **1** was added from a stock solution (1 mM in  $\text{H}_2\text{O}/\text{DMSO}$ ) after formation of the lipid vesicles. To check the influence of DMSO the corresponding amount of DMSO without **1** was added.

Small-angle X-ray scattering (SAXS) measurements were performed at the European Molecular Biology Laboratory (EMBL) beam line X33 at DESY/HASYLAB (Deutsches Elektronen-Synchrotron in Hamburg, Germany) with a wavelength  $\lambda = 0.15$  nm and covered a scattering vector range  $q = 1/d = (2 \sin \theta)/\lambda$  ( $2\theta$  = scattering angle,  $d$  = lattice spacing) from 0.1 to 3.5  $\text{nm}^{-1}$ . The samples were prepared on site just in time for the measurements, filled into copper cuvettes (with capton windows, 60  $\mu\text{L}$ ), and measured in a temperature-controlled sample holder. The temperature was varied from 7 to 50 °C at 1 °C/min. Data were collected for 30 s per measurement. Before and after each temperature ramp, the solvent was measured as background. The calibration for the SAXS spectra was done by measuring rat tail cornea (repeat distance 65 nm) in addition to silver behenate ( $[\text{CH}_3(\text{CH}_2)_{20}\text{COO}-\text{Ag}]$ , repeat distance 5.838 nm). The data were normalized with respect to the primary beam. Background subtraction was performed using a program supplied by A. Meyer, beam line A2, DESY, HASYLAB. The positions of the diffraction peaks were determined by the OTOKO software.<sup>49</sup>

## Results and Discussion

**Vesicle Leakage.** Large unilamellar vesicles (LUVs) containing calcein were prepared according to standard procedures. Two different types of LUVs were examined in which the total concentration of negative lipid was held constant at 10 mol %. Each LUV was composed of two lipids with one being zwitterionic (PE or PC) and the other being net negative (PG or PS). The two systems, PG-PE and PS-PC, contain lipids predominately found in bacterial and mammalian cell mem-



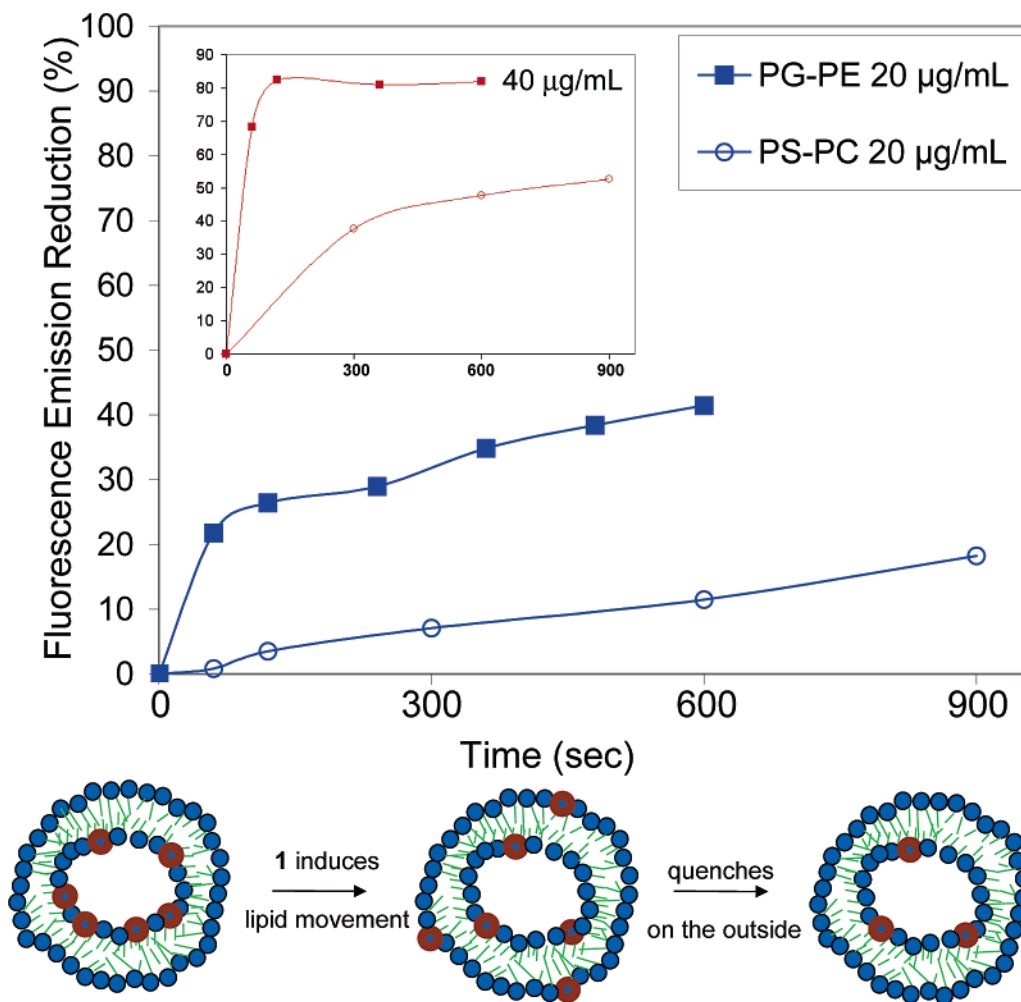


**Figure 3.** Vesicles containing fluorescent labels prepared so that the label is confined to the interior. Addition of **1** causes a reduction in fluorescence intensity due to the movement of the labeled lipid to the exterior followed by irreversible quenching from sodium hydrosulfite present in the surrounding solution. The inset shows additional quenching when the amount of **1** is increased to 40  $\mu\text{g/mL}$ . The curve shows that the PG-PE vesicles experience more quenching than the PS-PC vesicles.

branes, respectively. Keeping the overall net charge constant at 10 mol % negative allows the influence of lipid composition to be studied as opposed to electrostatics. When leakage experiments were performed on these two systems, the level of leakage imposed by the addition of **1** was significantly different. As shown in Figure 2, the leakage of PG-PE LUVs is concentration-dependent, in agreement with previous literature reports on HDPs and their mimics.<sup>6,10,42,43,50</sup> Complete leakage is obtained at 100  $\mu\text{g/mL}$ . More interestingly, striking differences are observed when PG-PE and PS-PC vesicles are compared. At 20  $\mu\text{g/mL}$ , 12% leakage is measured for PG-PE vesicles, compared to only 3% leakage for the PS-PC system at 10-fold higher concentrations. This shows dramatically that overall charge density is not the critical factor in determining selectivity for **1** in model vesicles and suggests that the phospholipid headgroup composition plays a critical role.

**Lipid Movement.** The results reported in Figure 2 demonstrate the ability to cause dye leakage in LUVs. Alternatively, the movement of lipids between the inner and outer leaflet of the bilayers is a highly controlled process in living organisms. Vesicle membranes are dynamic systems where the lipids are in motion and have the ability to move within a single leaflet relatively fast, but the movement across bilayers is minimal due to the unfavorable passage of the hydrophilic headgroup across the hydrophobic membrane core.<sup>18,51</sup> The addition of HDPs has been shown to promote rapid lipid movement across the

membrane.<sup>43,51–53</sup> This type of promoted lipid movement, which is not controlled by the host cell, would likely have serious consequences. To explore the ability of **1** to promote lipid movement across the bilayer, LUVs were prepared with fluorescently labeled lipids initially confined to the inner leaflet. If the addition of FA molecules causes lipids to move from the inner to the outer leaflet, the fluorescence would be irreversibly quenched due to the presence of sodium hydrosulfite in the solution. This is a sensitive technique to examine lipid-compound interactions.<sup>43,51</sup> Figure 3 shows the reduction in fluorescence emission of vesicles when exposed to 20  $\mu\text{g/mL}$  of **1**. The ability of **1** to act more strongly and quickly against PG-PE than PS-PC vesicles is observed again. This suggests that the activity of these biomimetic structures in both leakage and lipid movement experiments are more sensitive to lipid headgroup composition than the overall surface charge of the vesicle.

**In Vitro Dye Leakage.** Model membranes are significantly simpler than living organisms in many respects, the least of which is lipid composition. As a result, caution is always necessary in extrapolating observations with model vesicles to in vitro activity. Therefore, the ability of **1** to interact directly with the plasma membrane of living bacteria was explored. Specifically, *S. aureus* was incubated in the presence of diSC3-5 until the decrease in fluorescence, due to quenching, stabilized. After the removal of excess dye, the increase in fluorescence

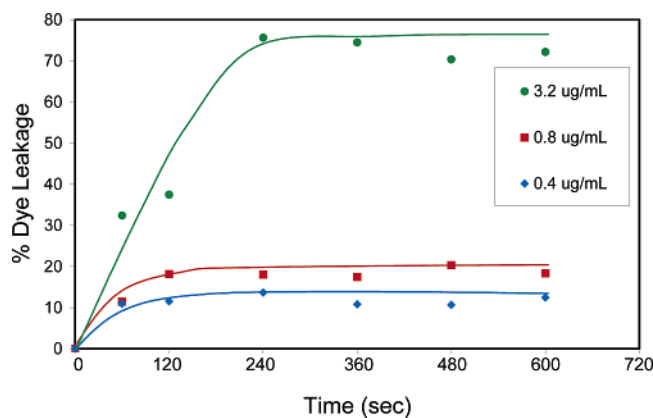


**Figure 4.** Dose-dependent leakage of the membrane-potential-sensitive cyanine dye, diSC3-5, from *S. aureus* in the presence of **1**. Leakage is observed for concentrations as low as 0.25 times the MIC. Considerable leakage (>70%) is observed at 2 times the MIC compared to many host defense peptides that typically require 4–10 times their respective MIC values. The model membrane studies and these in vitro leakage experiments occur on similar time scales.

intensity was monitored at different concentrations of **1** as shown in Figure 4. The increase in fluorescence is due to release of diSC3-5 from the membrane as the osmotic potential is reduced upon introduction of **1**. From this curve, it is clear that **1** is membrane-active against bacteria and induces dye leakage at concentrations very similar to the MIC. The similarities in dose-dependent leakage and kinetics between the vesicle and in vitro experiments support the further use of model membranes to investigate the interactions between these FA biomimetics and lipids.

The total concentration of **1** used in the model vesicle and in vitro experiments is different due to the overall concentration of phospholipids present in the two types of experiments. The in vitro experiments use a reduced number of bacteria compared to lipid vesicles. Current experiments are underway to understand the impact of vesicle concentration on overall leakage, but it is clear that concentration is important. This is consistent with the proposed mechanism, which involves binding of multiple molecules to a single vesicle or bacterium. The ability of **1** to cause leakage from *S. aureus* below the MIC indicates that this biomimetic is strongly membrane-active. Dye leakage below the MIC is expected if the compound is strongly membrane-active since this technique measures fluorescence, even from a few percentages of cells, while the MIC requires a greater than 90% reduction in cell count. In comparison, many HDPs do not show significant leakage until 4–10 times their

MIC, and the popular Polymyxin B does not show leakage until 50 times the MIC.<sup>44,45,54,55</sup> These differences may be important in determining the main mode of action for these novel molecules.

**Lipid Organization.** The above experiments established the membrane activity of **1** but focused almost exclusively on macroscopic solution properties (multiple fluorescent events). For example, dye leakage can be measured, but the lipid structure remains unknown. Combining these experiments with techniques to investigate molecule–lipid interactions on the molecular scale will provide a more comprehensive picture. As a result, the ability of these FA biomimetics to influence the order and ordering transition temperatures of lipids has been explored by SAXS, a powerful technique used frequently to study structural alterations caused by membrane-active molecules.<sup>56</sup> As the first test system, stearyl-oleoyl-phosphatidylserine (SOPS) was chosen because a strong charge-driven interaction can be expected; however, the experiments described above showed so little interaction with the PS–PC systems that it was unknown if **1** would even bind to PS. In addition, SOPS shows a phase transition in the experimentally accessible temperature range, unlike 1-palmitoyl-2-oleoyl-phosphatidyl-glycerol (POPG) which is found only in the liquid crystalline (LC) phase for temperatures above  $-2^{\circ}\text{C}$ , making SOPS an ideal starting point for these SAXS experiments.

Figure 5 compares the order of SOPS in the absence and presence of **1**. From these diffraction studies, the presence of **1** has a significant impact on the ordering of SOPS. The lipid SOPS forms vesicles with a repeat distance of 5.3 nm at  $20^{\circ}\text{C}$  and switches from a gel phase into the LC phase at  $17^{\circ}\text{C}$ . Upon the addition of **1**, the shape of the scattering curves changed dramatically, as shown in Figure 5b, suggesting that **1** induces highly ordered lamellar lipid structures, consistent with the sharp diffraction peaks. Two sets of diffraction peaks are present, indicating a coexistence of the gel and the LC phase. In addition, SOPS vesicles in the absence of **1** complete the phase transition within a  $5^{\circ}\text{C}$  temperature window, in sharp contrast to the sample containing **1**, in which this transition is prolonged up to nearly  $30^{\circ}\text{C}$ . This suggests that the presence of **1** almost completely hinders the phase transition from the gel to LC phase. These experiments show that **1** interacts strongly with pure SOPS phases, as would be expected since the two structures are oppositely charged. The lack of activity against the PS–PC vesicles is likely due to the dilution of PS with PC, and this is supported by a series of mixed lipid experiments in which the concentration of PS to PC is varied.<sup>57</sup> At small PS-to-PC ratios, limited interactions with **1** are observed; however, as the

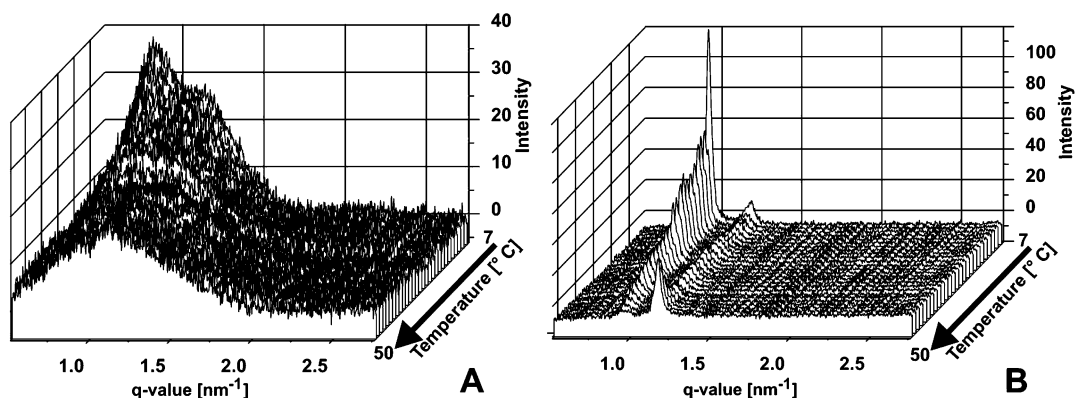


**Figure 5.** Temperature-dependent SAXS spectra for (left) SOPS and (right) SOPS with high concentrations of **1** (10:1; lipid/**1**). The presence of **1** induces SOPS to form multilamellar vesicles giving rise to considerably sharper diffraction curves. In addition, the phase transition is completely hindered at  $17^{\circ}\text{C}$  and shifted by almost  $30^{\circ}\text{C}$  toward higher values in the presence of **1**.

amount of PS is increased stronger interactions are measured. This study shows that **1** will bind with PS headgroups but that the interaction can be controlled by decreasing the concentration of PS. This is in agreement with the biological selectivity of **1**, which shows limited disruption of RBCs. It is well-known that the PS headgroup is only found to a minor extent in eukaryotic cell membranes and usually confined to the inner leaflet.<sup>39</sup> The SAXS studies have been extended to examine the interaction of **1** with PC and PE lipids.<sup>57</sup>

## Conclusions

The interaction of novel FA biomimetic molecules with phospholipid bilayers showed that the lipid headgroup and the concentration of lipid molecules within the bilayer have a significant impact on overall activity. PG–PE vesicles are significantly more sensitive to these molecules than the corresponding PS–PC vesicles, although the overall net charge is identical. Both leakage and lipid movement are more sensitive for PG–PE compared to PS–PC vesicles. In vitro experiments on *S. aureus* showed that these molecules are active against living bacterial membranes at the MIC concentrations and active on similar time scales to the vesicle experiments. This provides good support for using model membranes to investigate lipid interactions of these novel molecules. SAXS allows studying of the order and phase transition temperatures in the presence of these molecules. Applying a variety of analytical tools will be essential to gaining further insight on how these novel biomimetics interact with lipids and provide experimental details for improved computational efforts.

**Acknowledgment.** We gratefully acknowledge the help of D. Svergun and M. Rössle, beamline scientists at the EMBL SAXS beamline in Hamburg at HASYLAB, DESY, and M. Kumpugdee Vollrath, B. Krause-Kyora, O. Bruns, and J.-H. Hehemann. G.N.T gratefully acknowledges the National Institutes of Health for generous support (RO1-GM-65803) as well as the PECASE program, ARO and ONR for Young Investigator Awards, NSF-CAREER, 3M Nontenured Faculty Award, and DuPont Young Faculty Grant.

## References and Notes

- Cheng, R. P.; Gellman, S. H.; DeGrado, W. F. *Chem. Rev.* **2001**, *101*, 3219.
- Porter, E. A.; Wang, X. F.; Lee, H. S.; Weisblum, B.; Gellman, S. H. *Nature* **2000**, *404*, 565.
- Raguse, T. L.; Porter, E. A.; Weisblum, B.; Gellman, S. H. *J. Am. Chem. Soc.* **2002**, *124*, 12774.
- Porter, E. A.; Weisblum, B.; Gellman, S. H. *J. Am. Chem. Soc.* **2002**, *124*, 7324.
- Hamuro, Y.; Schneider, J. P.; DeGrado, W. F. *J. Am. Chem. Soc.* **1999**, *121*, 12200.
- Liu, D. H.; DeGrado, W. F. *J. Am. Chem. Soc.* **2001**, *123*, 7553.
- Patch, J. A.; Barron, A. E. *J. Am. Chem. Soc.* **2003**, *125*, 12092.
- Fernandez-Lopez, S.; Kim, H. S.; Choi, E. C.; Delgado, M.; Granja, J. R.; Khasanov, A.; Kraehenbuehl, K.; Long, G.; Weinberger, D. A.; Wilcoxon, K. M.; Ghadiri, M. R. *Nature* **2001**, *412*, 452.
- Oren, Z.; Shai, Y. *Biochemistry* **1997**, *36*, 1826.
- Tew, G. N.; Liu, D. H.; Chen, B.; Doerksen, R. J.; Kaplan, J.; Carroll, P. J.; Klein, M. L.; DeGrado, W. F. *Proc. Natl. Acad. Sci. U.S.A.* **2002**, *99*, 5110.
- Arnt, L.; Nusslein, K.; Tew, G. N. *J. Polym. Sci., Polym. Chem.* **2004**, *42*, 3860.
- Chen, X.; Tang, H.; Even, M. A.; Wang, J.; Tew, G. N.; Chen, Z. *J. Am. Chem. Soc.* **2006**, in press.
- Tang, H.; Doerksen, R. J.; Tew, G. N. *Chem. Commun.* **2005**, 1537.
- Ilker, M. F.; Nusslein, K.; Tew, G. N.; Coughlin, E. B. *J. Am. Chem. Soc.* **2004**, *126*, 15870.
- Arnt, L.; Tew, G. N. *J. Am. Chem. Soc.* **2002**, *124*, 7664.
- Arnt, L.; Tew, G. N. *Langmuir* **2003**, *19*, 2404.
- Lehrer, R. I.; Lichtenstein, A. K.; Ganz, T. *Annu. Rev. Immunol.* **1993**, *11*, 105.
- Alberts, B.; Bray, D.; Lewis, J.; Raff, M.; Roberts, K.; Watson, J. D. *Molecular Biology of the Cell*, 3rd ed.; Garland Publishing: New York, 1994.
- Wikstrom, M.; Xie, J.; Bogdanov, M.; Mileykovskaya, E.; Heacock, P.; Wieslander, A.; Dowhan, W. *J. Biol. Chem.* **2004**, *279*, 10484.
- Cronan, J. E. *Annu. Rev. Microbiol.* **2003**, *57*, 203.
- Matsukaki, K.; Sugishita, K.; Fujii, N.; Miyajima, K. *Biochemistry* **1995**, *34*, 3423.
- Matsuzaki, K. *Biochim. Biophys. Acta* **1999**, *1462*, 1.
- Wu, M.; Maier, E.; Benz, R.; Hancock, R. E. *Biochemistry* **1999**, *38*, 7235.
- Tajkhorshid, E.; Nollert, P.; Jensen, M. O.; Miercke, L. J. W.; O'Connell, J.; Stroud, R. M.; Schulten, K. *Science* **2002**, *296*, 525.
- Khandelia, H.; Kaznessis, Y. N. *J. Phys. Chem. B* **2005**, *109*, 12990.
- Kandasamy, S. K.; Larson, R. G. *Chem. Phys. Lipids* **2004**, *132*, 113.
- Shepherd, C. M.; Vogel, H. J.; Tieleman, D. P. *Biochem. J.* **2003**, *370*, 233.
- La Rocca, P.; Shai, Y.; Sansom, M. S. P. *Biophys. Chem.* **1999**, *76*, 145.
- Lopez, C. F.; Nielsen, S. O.; Moore, P. B.; Klein, M. L. *Proc. Natl. Acad. Sci. U.S.A.* **2004**, *101*, 4431.
- Nielsen, S. O.; Lopez, C. F.; Srinivas, G.; Klein, M. L. *J. Phys.: Condens. Matter* **2004**, *16*, R481.
- Srinivas, G.; Klein, M. L. *Nanotechnology* **2004**, *15*, 1289.
- Saiz, L.; Klein, M. L. *Acc. Chem. Res.* **2002**, *35*, 482.
- Saiz, L.; Bandyopadhyay, S.; Klein, M. L. *J. Phys. Chem. B* **2004**, *108*, 2608.
- Tossi, A.; Sandri, L.; Giangaspero, A. *Biopolymers* **2000**, *55*, 4.
- Graham, J. M. *Membrane Analysis*; Springer: New York, 1997.
- Ratledge, C.; Wilkinson, S. G. *Microbial Lipids*; Academic Press: London, 1988.
- Madigan, M. T.; Martinko, J. M.; Parker, J. *Brock Biology of Microorganisms*, 10th ed.; Pearson Education: Upper Saddle River, NJ, 2003.
- Nouri-Sorkhabi, M. H.; Wright, L. C.; Sullivan, D. R.; Gallagher, C.; Kuchel, P. W. *Lipids* **1996**, *31*, 756.
- Lohner, K.; Prenner, E. J. *Biochim. Biophys. Acta* **1999**, *1462*, 141.
- Rennie, J.; Arnt, L.; Tang, H.; Nusslein, K.; Tew, G. N. *J. Ind. Microbiol. Biotechnol.* **2005**, *32*, 296.
- Wilschut, J.; Duzgunes, N.; Fraley, R.; Papahadjopoulos, D. *Biochemistry* **1980**, *19*, 6011.
- Gazit, E.; Boman, A.; Boman, H. G.; Shai, Y. *Biochemistry* **1995**, *34*, 11479.
- Matsukaki, K.; Murase, O.; Fujii, N.; Miyajima, K. *Biochemistry* **1996**, *35*, 11361.
- Zhang, L.; Scott, M. G.; Yan, H.; Mayer, L. D.; Hancock, R. E. *Biochemistry* **2000**, *39*, 14504.
- Friedrich, C. L.; Moyles, D.; Beveridge, T. J.; Hancock, R. E. *Antimicrob. Agents Chemother.* **2000**, *44*, 2086.
- Ehringer, W. D.; Su, S.; Chiang, B.; Stillwell, W.; Chien, S. *Lipids* **2002**, *37*, 885.
- Sims, P. J.; Waggoner, A. S.; Wang, C.-H.; Hoffman, J. F. *Biochemistry* **1974**, *13*, 3315.
- Ghazizadeh, A.; Schechter, E.; Letellier, L.; Labedan, B. *FEBS Lett.* **1981**, *125*, 197.
- Boulin, C.; Kempf, R.; Koch, M. H. J.; McLaughlin, S. M. *Nucl. Instrum. Methods Phys. Res., Sect. A* **1986**, *249*, 399.
- Matsuzaki, K.; Harada, M.; Handa, T.; Funakoshi, S.; Fujii, N.; Yajima, H.; Miyajima, K. *Biochim. Biophys. Acta* **1989**, *981*, 130.
- Zhang, L.; Rozek, A.; Hancock, R. E. *J. Biol. Chem.* **2001**, *276*, 35714.
- Epand, R. F.; Umezawa, N.; Porter, E. A.; Gellman, S. H.; Epand, R. M. *Eur. J. Biochem.* **2003**, *270*, 1240.
- Kol, M. A.; van Dalen, A.; de Kroon, A. I. P. M.; de Kruijff, B. *J. Biol. Chem.* **2003**, *278*, 24586.
- Zhang, L.; Dillon, P.; Yan, H.; Farmer, S.; Hancock, R. E. *Antimicrob. Agents Chemother.* **2000**, *44*, 3317.
- Anderson, R. C.; Hancock, R. E.; Yu, R.-L. *Antimicrob. Agents Chemother.* **2004**, *48*, 673.
- Willumeit, R.; Kumpugdee, M.; Funari, S. S.; Lohner, K.; Pozo Navas, B.; Brandenburg, K.; Linser, S.; Andrä, J. *Biochim. Biophys. Acta* **2005**, *1669*, 125–134.
- Willumeit, R.; Tew, G. N. Unpublished work.